Optical Engineering

SPIEDigitalLibrary.org/oe

# Range estimation of passive infrared targets through the atmosphere

Hoonkyung Cho
Joohwan Chun
Doochun Seo
Seokweon Choi

Optical Engineering 52(4), 046402 (April 2013)

# Range estimation of passive infrared targets through the atmosphere

**Hoonkyung Cho**
**Joohwan Chun**
Korea Advanced Institute of Science and Technology
Department of Electrical Engineering
Daejeon, Republic of Korea
E-mail: hkcho@sclab.kaist.ac.kr

**Doochun Seo**
**Seokweon Choi**
Korea Aerospace Research Institute
169-84, Gwahak-ro, Yuseong-gu
Daejeon, Republic of Korea

**Abstract.** Target range estimation is traditionally based on radar and active sonar systems in modern combat systems. However, jamming signals tremendously degrade the performance of such active sensor devices. We introduce a simple target range estimation method and the fundamental limits of the proposed method based on the atmosphere propagation model. Since passive infrared (IR) sensors measure IR signals radiating from objects in different wavelengths, this method has robustness against electromagnetic jamming. The measured target radiance of each wavelength at the IR sensor depends on the emissive properties of target material and various attenuation factors (i.e., the distance between sensor and target and atmosphere environment parameters). MODTRAN is a tool that models atmospheric propagation of electromagnetic radiation. Based on the results from MODTRAN and atmosphere propagation-based modeling, the target range can be estimated. To analyze the proposed method's performance statistically, we use maximum likelihood estimation (MLE) and evaluate the Cramer-Rao lower bound (CRLB) via the probability density function of measured radiance. We also compare CRLB and the variance of MLE using Monte-Carlo simulation.  [DOI: 10.1117/1.OE.52.4.046402]

Subject terms: range estimation; atmospheric attenuation; MODTRAN; atmospheric transmittance; maximum likelihood estimation; Cramer-Rao lower bound; passive infrared sensor; distance estimation.

Paper 121129PRR received Aug. 7, 2012; revised manuscript received Mar. 12, 2013; accepted for publication Mar. 12, 2013; published online Apr. 22, 2013.

## 1 Introduction

The infrared (IR) sensor, which measures light intensity impinging on it, has traditionally been used to detect a target or to image an object located at a remote distance. To analyze the detection performance or the signal-to-noise ratio (SNR) of the IR image, researchers[1,2] have investigated the relationship among the target range, the target radiance, and the SNR, where the SNR (or the detection probability) is the main parameter of interest, and the target range is usually treated as a known input parameter. In this paper, we treat the target range as a parameter to be estimated and the received radiance of the target at the sensor as measurement. Therefore, we use an IR sensor to measure the distance passively, unlike previous approaches,[3–5] where the range was estimated using the reflected IR signal with an illuminating IR source.

To estimate the target range from the received IR radiance at the sensor, we need to know the emitted radiance at the target, as well as the atmospheric propagation information, i.e., transmittance, sky radiance, and path radiance. The emitted radiance is a function of temperature and material properties, such as the emissivity of the target surface. In this paper, target temperature is assumed to be known. For a rapidly approaching target, however, target temperature can also be estimated using target aerodynamic information by solving the differential equation[6,7] that governs heat conduction, convection, and radiation. The heat source could be the irradiance on the target due to solar and sky radiance, as well as the frictional dissipation.

Modeling the transmittance, sky radiance, and path radiance is difficult, because they are dependent on numerous time-varying atmospheric parameters that are not easy to determine. A usual practice is to utilize the widely accepted MODTRAN[8] software, which models the atmosphere as a number of homogenous layers that can be solved individually.

In this paper, we shall derive the maximum likelihood estimate (MLE) $\hat{d}$ of the range and the Cramer-Rao lower bound (CRLB)—the lowest possible mean squared error for the passive range estimation problem. Our analysis indicates that the passive ranging gives reasonably accurate range estimation when target temperature, range, and emissivity are more than 500 K, 2000 m, and 0.7, respectively.

The measurement model used by MODTRAN is explained in Sec. 2. The CRLB for the passive range estimate is derived in Sec. 3, and simulation study is shown in Sec. 4. Our conclusion is made in Sec. 5.

## 2 Measurement Model

### 2.1 *Atmospheric Transmittance*

The atmosphere consists of innumerable aerosol and gas particles that scatter and absorb radiation. The atmospheric transmittance $\tau(\lambda, d)$, where $d$ is the range from the sensor to the target, is the capacity of the atmosphere to transmit electromagnetic energy, which is modeled as a $d$'th power of the transmittance per unit distance $\tau(\lambda)$, so that

$$\tau(\lambda, d) = \tau^d(\lambda), \qquad \tau(\lambda) = e^{-\gamma(\lambda)}$$

$$\gamma(\lambda) = \sigma(\lambda) + k(\lambda),$$

where $\sigma(\lambda)$ and $k(\lambda)$ are the scattering component and the absorptive component, respectively. If light travels through atmosphere of thickness $d$, the resulting radiance value will be attenuated by the factor of $\tau(\lambda, d)$. Typical atmospheric transmittances obtained with MODTRAN 4.0 for varying distances are illustrated in Fig. 1.

### 2.2 *Radiance Measurement Model*

Assuming there is no scattering into the line of sight, the received radiance at the sensor would have three spectral radiance components: the self emission $L_T(\lambda)$, the reflected ambient radiance $L_{AE}(\lambda)$, and the path radiance $L_{\text{path}}(\lambda)$. If the IR sensor is responsive in a band of spectrum $[\lambda_{\min}, \lambda_{\max}]$, then the total radiance power that the sensor would receive will be

$$L = \int_{\lambda_{\min}}^{\lambda_{\max}} L_T(\lambda) + L_{AE}(\lambda) + L_{\text{path}}(\lambda)\mathrm{d}\lambda. \tag{1}$$

Each of the three contributions will be explained in detail below.

#### 2.2.1 *Self-emission*

Black body radiation is a type of electromagnetic radiation within or surrounding a body in thermodynamic equilibrium with its environment. The radiation has a specific spectrum and intensity that depends only on the body's temperature.[9] The spectral radiance of an ideal black body with a temperature $T_T$ follows Planck's black body radiation law; that is,

$$L_{\text{bb}}(\lambda, T) = \frac{c_1}{\lambda^5}\left(\frac{1}{e^{c_2/\lambda T} - 1}\right)[\mathrm{W/m^2/\mu m}],$$

where $c_1 = 3.7411 \times 10^8\ \mathrm{W}\,\mu\mathrm{m}^4/\mathrm{m}^2$, $c_2 = 1.4388 \times 10^4\ \mu\mathrm{m\,K}$, and $l$ is the wavelength in micrometers. A target with temperature $T_T$ can be modeled approximately as a gray body having the spectral radiance $\varepsilon(\lambda)L_{\text{bb}}(\lambda, T_T)$, where $\varepsilon(\lambda)$ is the spectral emissivity of the target. If the target is located in the range $d$ from the sensor, then the received spectral radiance at the sensor will be

$$L_T(\lambda) = \varepsilon(\lambda)\tau^d(\lambda)L_{\text{bb}}(\lambda, T_T). \tag{2}$$

Therefore,

$$L_T = \int_{\lambda_{\min}}^{\lambda_{\max}} L_T(\lambda)\mathrm{d}\lambda \approx \sum_{k=1}^{K} \varepsilon(\lambda_k)\tau^d(\lambda_k)L(\lambda_k, T_T)\Delta\lambda_k. \tag{3}$$

The summation approximation in Eq. (3) is more useful, because MODTRAN can provide transmittance only in discrete steps of spectrum. The general attenuation trend of black body radiation as a function of range is depicted in Fig. 2. Note that $d$ can be found accurately from Eq. (2) if $L_T$, $\tau(\lambda_k)$, and $T_T$ are known.

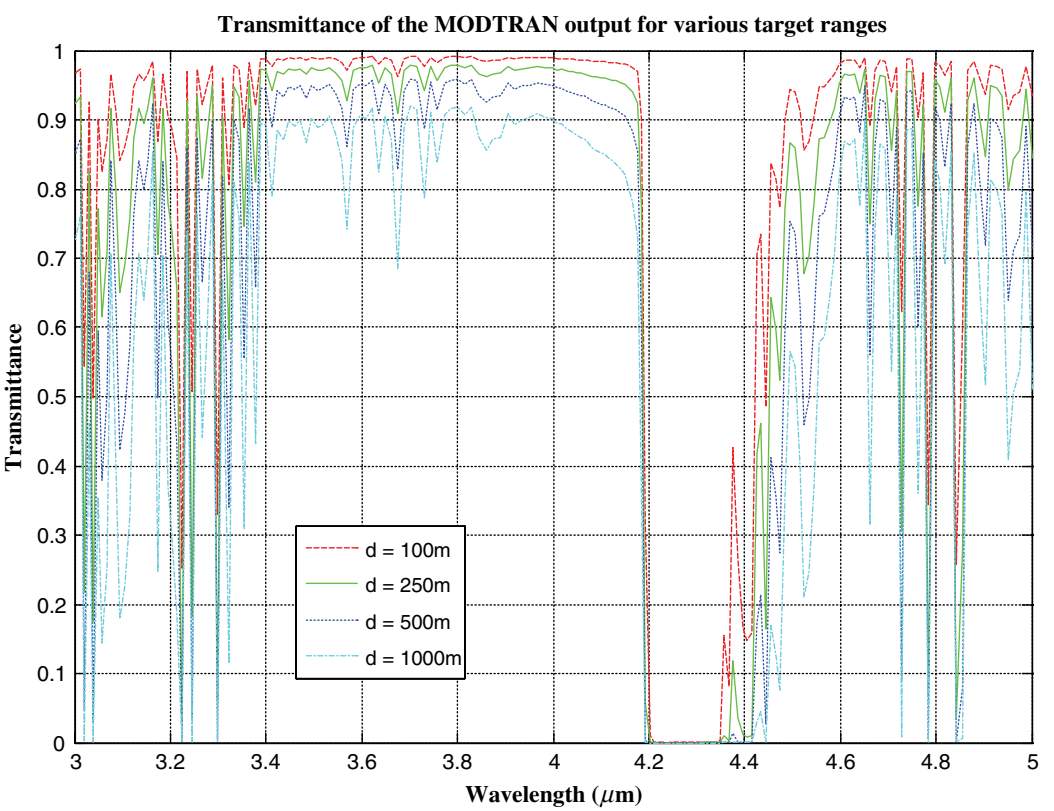


**Fig. 1** Typical atmospheric transmittance obtained with MODTRAN 4.0 for different target sensor distances, $d = 100$, 250, 500, and 1000 m.

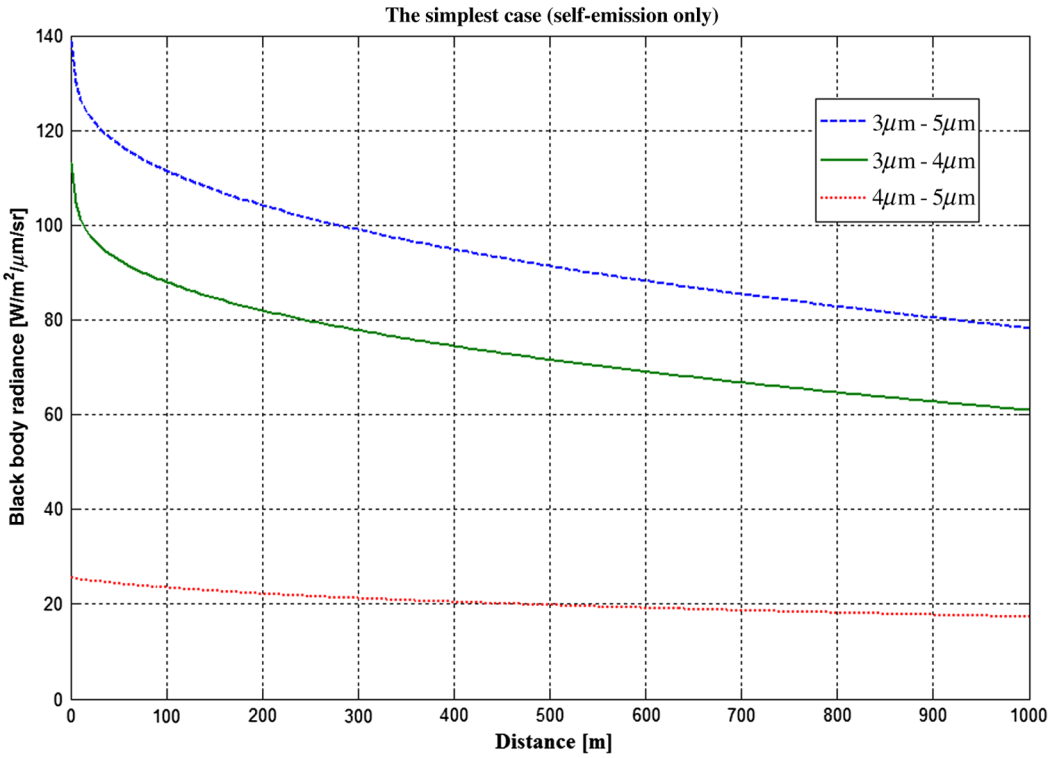


**Fig. 2** Radiance-to-distance curve in only the surface-emitted case, $\lambda_1 - \lambda_2 = 3$ to 5 mm, 3 to 4 mm, and 4 to 5 mm.

### 2.2.2 *Reflected ambient radiance*

Another contribution is the ambient down-welling radiation due to the atmosphere that reaches the target surface and is reflected toward the sensor. Assuming the atmosphere is a stack of up to $N$ semi-transparent layers, the down-welling radiation $L-_{,n}$ of the $n$'th layer toward the target can be expressed as

$$L_{\downarrow,n}(\theta,\phi) = L_{\mathrm{bb}}(\lambda, T_n)[1-\tau_{\downarrow,n}(\lambda)]\prod_{j=1}^{n-1}\tau_{\downarrow,j}(\lambda),$$

where $T_n$ is the temperature of the $n$'th layer, $\tau_{\downarrow,n}(\lambda) =$ transmittance through the $n$'th layer, and $1-\tau_{\downarrow,n}(\lambda) =$ emissivity of the $n$'th layer by Kirchhoff's law, which links the layer emission to transmission. Therefore, the total down-welling irradiance $E_\downarrow$ is given by

$$E_\downarrow = \int_{2\pi} L_\downarrow(\theta,\phi)\cos\theta \mathrm{d}\omega_i,$$

where $L_\downarrow(\theta,\phi)$ is the total down-welling spectral radiance given as $L_\downarrow(\theta,\phi) = \sum_{n=1}^{N} L_{\downarrow,n}(\theta,\phi)$.

The light reflection behavior at a particular surface is characterized by the bidirectional reflectance distribution function (BRDF), which is denoted as $r_{\mathrm{BRDF}}(\lambda,\omega_i,\omega_r)$, where $\omega_i = (\theta,\phi)$ is the incident angle, and $\omega_r = (\theta',\phi')$ is the reflection angle. It is the ratio of the reflected radiance exiting along the reflect angle $w_r$ to the irradiance incident on the surface from the direction $w_i$. Therefore,

$$L_{\mathrm{bb}}(\lambda, T_{AE}) = \frac{E_\downarrow r_{\mathrm{BRDF}}(\lambda,\omega_i,\omega_r)}{\rho(\lambda)}, \tag{4}$$

where $\rho(\lambda) = 1-\varepsilon(\lambda)$ is the spectral reflectivity of the target, and $T_{AE}$ is the average downward environmental temperature. Therefore, the radiance that reach the sensor will be

$$L_{AE}(\lambda) = \rho(\lambda)\tau^d(\lambda)L_{\mathrm{bb}}(\lambda, T_{AE}). \tag{5}$$

### 2.2.3 *Path radiance*

Finally, we need to consider the path radiance emitted by the atmosphere in the path between the target and the IR sensor. With Kirchhoff's law, the path radiance can be written as

$$L_{\mathrm{bb}}(\lambda, T_{\mathrm{ATM}}) = \frac{L_\uparrow(\theta',\phi')}{1-\tau^d(\lambda)}, \tag{6}$$

where

$$\begin{aligned} L_\uparrow(\theta',\phi') &= \sum_{n=1}^{N} L_{\uparrow,n}(\theta',\phi'), \\ L_{\uparrow,n}(\theta',\phi') &= L_{\mathrm{bb}}(\lambda, T_n)[1-\tau_{\uparrow,n}(\lambda)]\prod_{j=1}^{n-1}\tau_{\uparrow,j}(\lambda), \end{aligned} \tag{7}$$

and $\tau_{\uparrow,n}(\lambda)$ is the transmittance from the target to the sensor through the $n$'th layer. Therefore, the radiance that reaches the sensor will be

$$L_{\text{path}}(\lambda) = [1 - \tau^d(\lambda)]L_{\text{bb}}(\lambda, T_{\text{ATM}}).$$

## 3 Maximum Likelihood Estimation and Performance Analysis

We shall show how to find the MLE $\hat{d}$ from the noise-corrupted radiance measurement $\tilde{L}$. Two types of noise (or uncertainty) are considered in this paper: the thermal noise[10,11] $v_{\text{thm}}$ generated in the sensor circuitry and the uncertainty in the emissivity $\varepsilon(\lambda)$. We assume that both are Gaussian distributed; that is,

$$\tilde{L} = L + v_{\text{thm}}, \qquad v_{\text{thm}} \sim N(0, \sigma_{\text{thm}}^2),$$

$$\tilde{\varepsilon}(\lambda) = \varepsilon(\lambda) + v_\varepsilon, \qquad v_\varepsilon \sim N(0, \sigma_\varepsilon^2).$$

Therefore, the measured radiance $\tilde{L}$ is given by

$$\begin{aligned}\tilde{L} = \int_{\lambda_{\min}}^{\lambda_{\max}} \{&[\tilde{\varepsilon}(\lambda)]\tau^d(\lambda)L_{\text{bb}}(\lambda, T_T) \\ &+ [1 - \tilde{\varepsilon}(\lambda)]\tau^d(\lambda)L_{\text{bb}}(\lambda, T_{AE}) \\ &+ [1 - \tau^d(\lambda)]L_{\text{bb}}(\lambda, T_{\text{ATM}})d\lambda\} + v_{\text{thm}}. \end{aligned} \tag{8}$$

To get the range estimate $\hat{d}$ from $\tilde{L}$, we first need to find the probability density function (PDF), $p(\tilde{L}|d)$. Note that the transformation from $v_e$ and $v_{\text{thm}}$ to $\tilde{L}$ is linear, which implies that $p(\tilde{L}|d)$ is Gaussian, because $v_e$ and $v_{\text{thm}}$ are Gaussian. Therefore, $p(\tilde{L}|d)$ is completely determined by its mean $\tilde{L}_\mu = E[\tilde{L}|d]$ and variance $\tilde{\sigma}^2 = \text{var}[\tilde{L}|d]$, which are given by

$$\begin{aligned}\tilde{L}_\mu = \int_{\lambda_{\min}}^{\lambda_{\max}} \{&\varepsilon(\lambda)\tau^d(\lambda)L_{\text{bb}}(\lambda, T_T) + \rho(\lambda)\tau^d(\lambda)L_{\text{bb}}(\lambda, T_{AE}) \\ &+ [1 - \tau^d(\lambda)]L_{\text{bb}}(\lambda, T_{\text{ATM}})\}\text{d}\lambda, \end{aligned} \tag{9}$$

$$\begin{aligned}\tilde{\sigma}^2 &= \sigma_{\text{thm}}^2 + \sigma_\varepsilon'^2, \sigma_\varepsilon'^2 \\ &= \sigma_\varepsilon^2\{\int_{\lambda_{\min}}^{\lambda_{\max}} \tau^d(\lambda)[L_{\text{bb}}(\lambda, T_T) - L_{\text{bb}}(\lambda, T_{AE})]\text{d}\lambda\}^2, \end{aligned} \tag{10}$$

assuming $v_e$ and $v_{\text{thm}}$ are uncorrelated. Note that $\sigma_\varepsilon'^2$ is a function of $d$. Therefore,

$$p(\tilde{L}|d) = \frac{1}{\sqrt{2\pi(\sigma_{\text{thm}}^2 + \sigma_\varepsilon'^2)}} \exp\left(-\frac{(\tilde{L} - \tilde{L}_\mu)^2}{2(\sigma_{\text{thm}}^2 + \sigma_\varepsilon'^2)}\right), \tag{11}$$

and

$$\ln\, p(\tilde{L}|d) = -\frac{1}{2}\ln[2\pi(\sigma_{\text{thm}}^2 + \sigma_\varepsilon'^2)] - \frac{(\tilde{L} - \tilde{L}_\mu)^2}{2(\sigma_{\text{thm}}^2 + \sigma_\varepsilon'^2)}. \tag{12}$$

Now the MLE $\hat{d}$ is the one that maximizes $p(\tilde{L}|d)$, which can be found by setting the derivative of $\ln\, p(\tilde{L}|d)$ to be zero; that is,

$$\begin{aligned}\frac{\partial \ln\, p(\tilde{L}|d)}{\partial d} = \frac{-\sigma_\varepsilon'}{(\sigma_{\text{thm}}^2 + \sigma_\varepsilon'^2)} \cdot \frac{\partial \sigma_\varepsilon'}{\partial d} + \Bigg[&\frac{(\tilde{L} - \tilde{L}_\mu)}{(\sigma_{\text{thm}}^2 + \sigma_\varepsilon'^2)} \\ &\cdot \frac{\partial \tilde{L}_\mu}{\partial d} + \frac{(\tilde{L} - \tilde{L}_\mu)^2}{(\sigma_{\text{thm}}^2 + \sigma_\varepsilon'^2)^2} \cdot \sigma_\varepsilon' \cdot \frac{\partial \sigma_\varepsilon'}{\partial d}\Bigg] = 0, \end{aligned} \tag{13}$$

where

$$\frac{\partial \sigma_\varepsilon'}{\partial d} = \sigma_\varepsilon^2 \int_{\lambda_{\min}}^{\lambda_{\max}} \ln[\tau(\lambda)]\tau^d(\lambda)[L_{\text{bb}}(\lambda, T_T) - L_{\text{bb}}(\lambda, T_{AE})]\text{d}\lambda, \tag{14}$$

$$\frac{\partial \tilde{L}_\mu}{\partial d} = \ln[\tau(\lambda)]\tilde{L}_\mu - \int_{\lambda_{\min}}^{\lambda_{\max}} L_{\text{bb}}(\lambda, T_{\text{ATM}})\text{d}\lambda. \tag{15}$$

Note that Eq. (13) is not linear and must be solved numerically. However, if $\sigma_\varepsilon^2 = 0$, then Eq. (13) reduces to

$$\frac{\tilde{L} - \tilde{L}_\mu}{\sigma_{\text{thm}}^2} = 0, i.e., \tilde{L} = \tilde{L}_\mu,$$

from which $\hat{d}$ can be found easily using Eq. (9).

Now, using Eq. (13) with Eqs. (14) and (15), we can obtain the CRLB by

$$\text{CRLB} = \frac{1}{E\left[\frac{\partial}{\partial d}\ln\, p(\tilde{L}|d)\right]^2}. \tag{16}$$

## 4 Simulation Results

We calculate the variance of MLE solution by Monte-Carlo simulation. We set the emissivity $e = 0.6, 0.7, 0.8, 0.9$, and the temperature $T_T = 450, 500, 550$, and 600 K, for various standard deviations in thermal noise $s_{\text{thm}} = 0.5, 1.0, 1.5, 2.0$, and in emissivity noise $s_e = 0.005, 0.010, 0.015, 0.020$.

### 4.1 *Effect of Thermal Noise*

The average and variance of maximum likelihood estimator $d_{\text{ML}}$ is evaluated 20,000 times in Monte-Carlo simulation via various standard deviations in thermal noise, temperature, and emissivity. The results of Monte-Carlo simulation shown in Figs. 3–5 are converged to CRLB, because the maximum likelihood estimator of the distance is efficient.

From Fig. 3, we see that the CRLB and the standard deviation of ML estimated distance to true distance curve for various thermal noise standard deviations. As the standard deviation in thermal noise $s_{\text{thm}}$ increases, the standard deviation of estimated distance also increases, and the detection performance decreases. As Figs. 4 and 5 show, the intense $L_{\text{detector}}$ causes better detection performance. In summary, as $s_{\text{thm}}$ increases, and the target temperature and emissivity decrease, the standard deviation of estimated distance and detection performance increases. Passive ranging gives reasonably accurate range estimation within a margin of error of 10% with a 95% confidence interval when the target temperature, range, standard deviation in thermal noise, and emissivity are more than 500 K, 2000 m, 1.0, and 0.7, respectively.

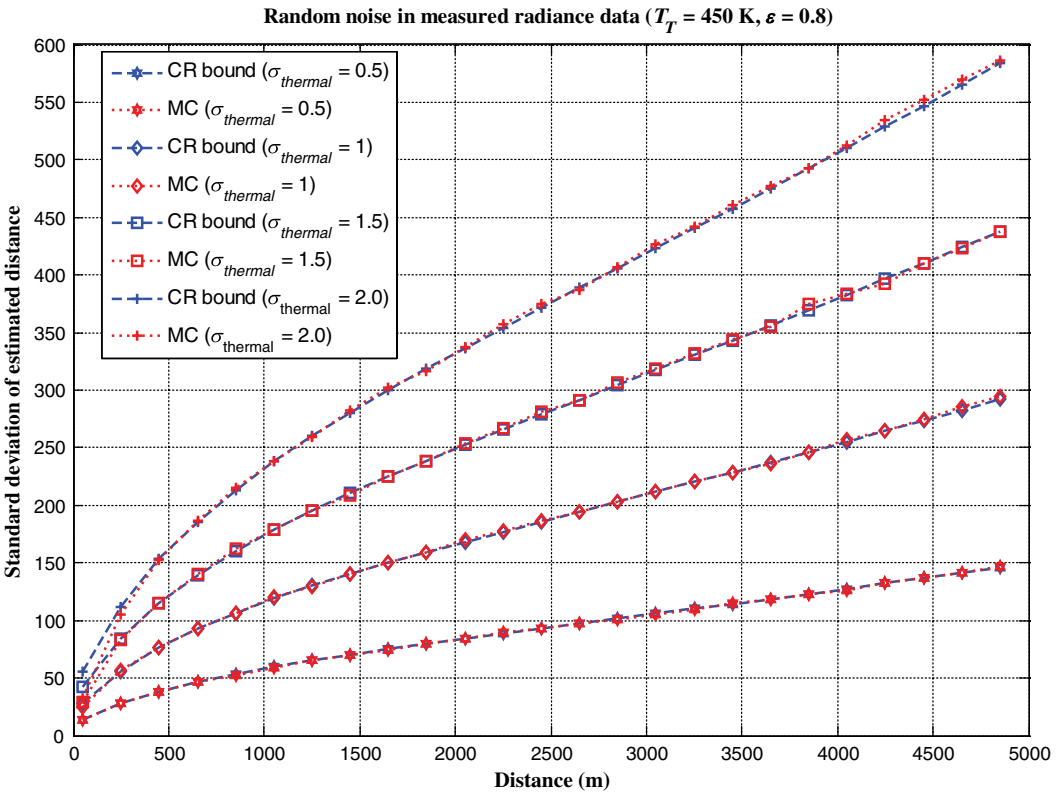


**Fig. 3** CRLB and standard deviation of ML estimated distance to distance curve in the thermal noise case, $s_{\text{thermal}} = 0.5$, 1.0, 1.5, and 2.0.

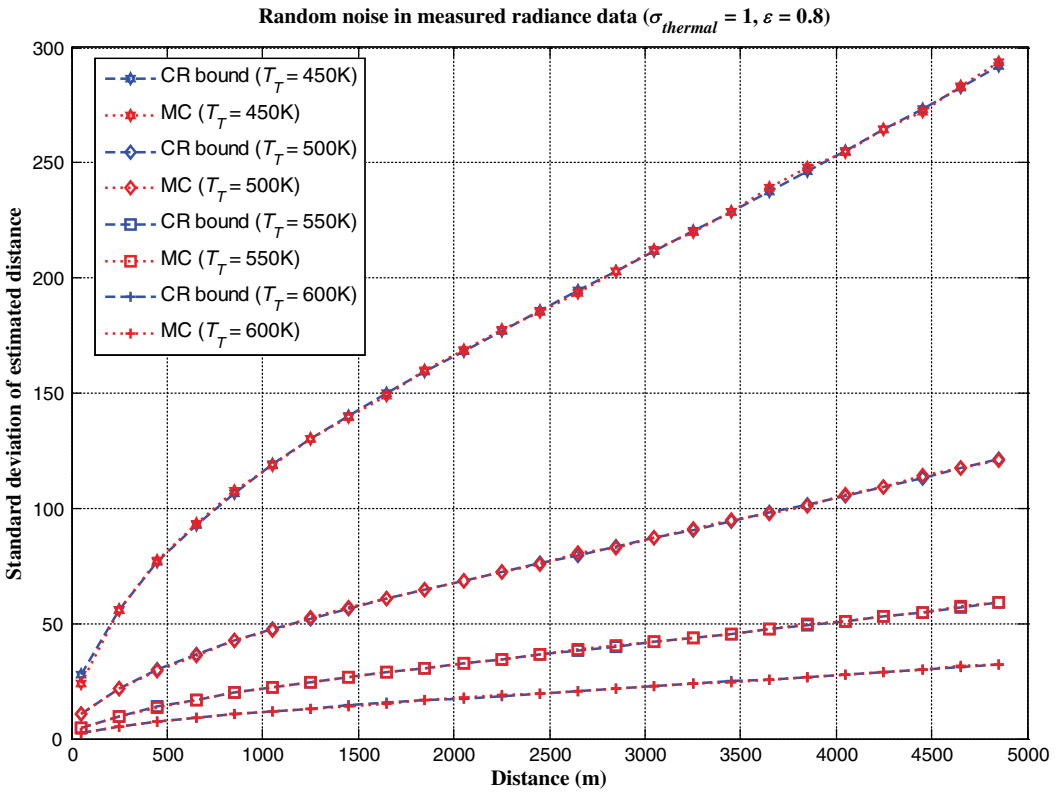


**Fig. 4** CRLB and standard deviation of ML estimated distance to distance curve in the thermal noise case, $T_T = 450$, 500, 550, and 600 K.

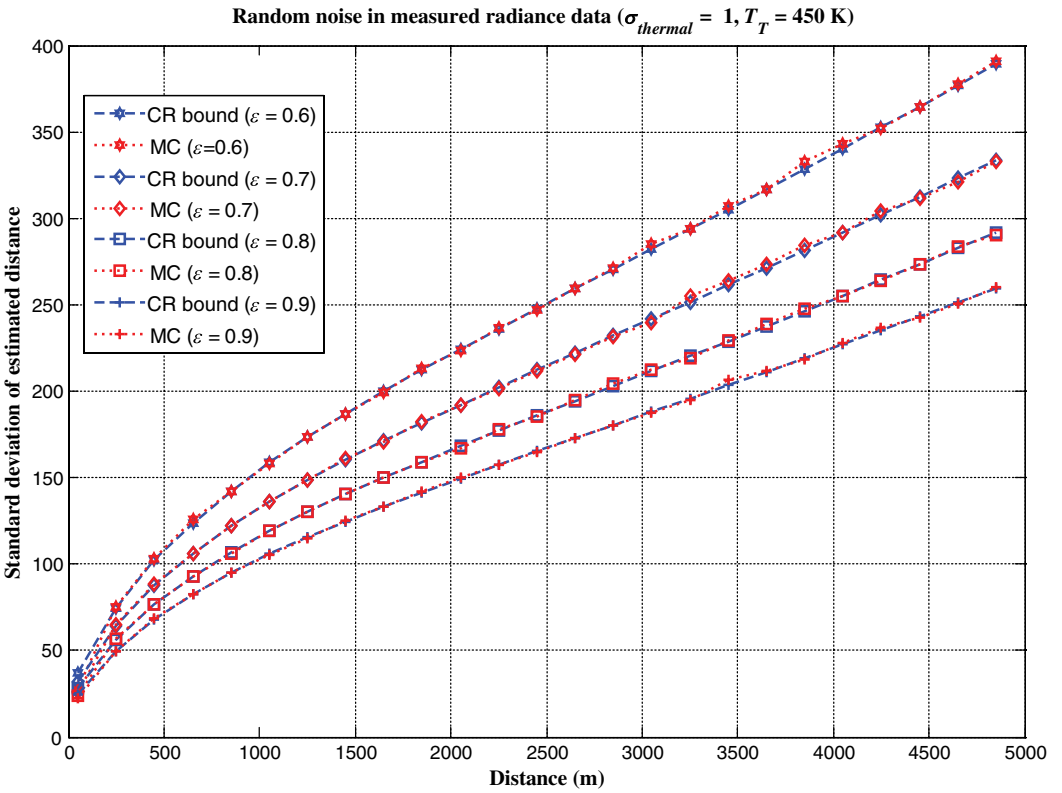


**Fig. 5** CRLB and standard deviation of ML estimated distance to distance curve in the thermal noise case, $e = 0.6$, 0.7, 0.8, and 0.9.

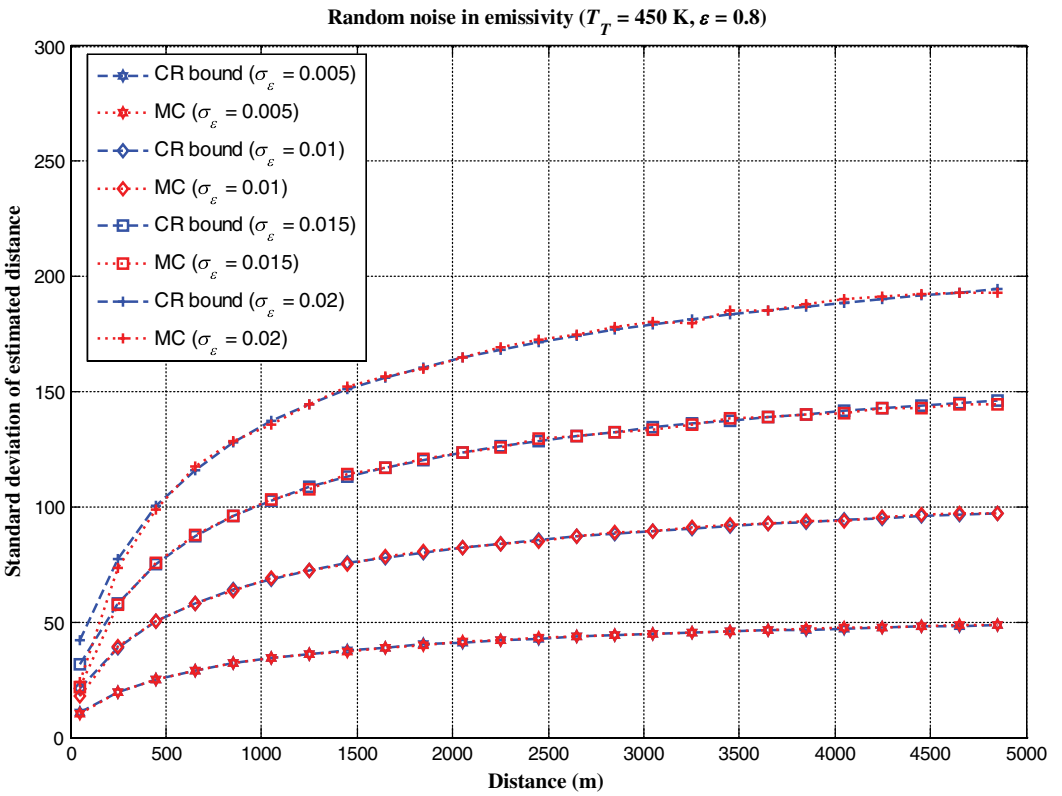


**Fig. 6** CRLB and standard deviation of ML estimated distance to distance curve in the emissivity uncertainty case, $s_e = 0.005$, 0.01, 0.015, and 0.02.

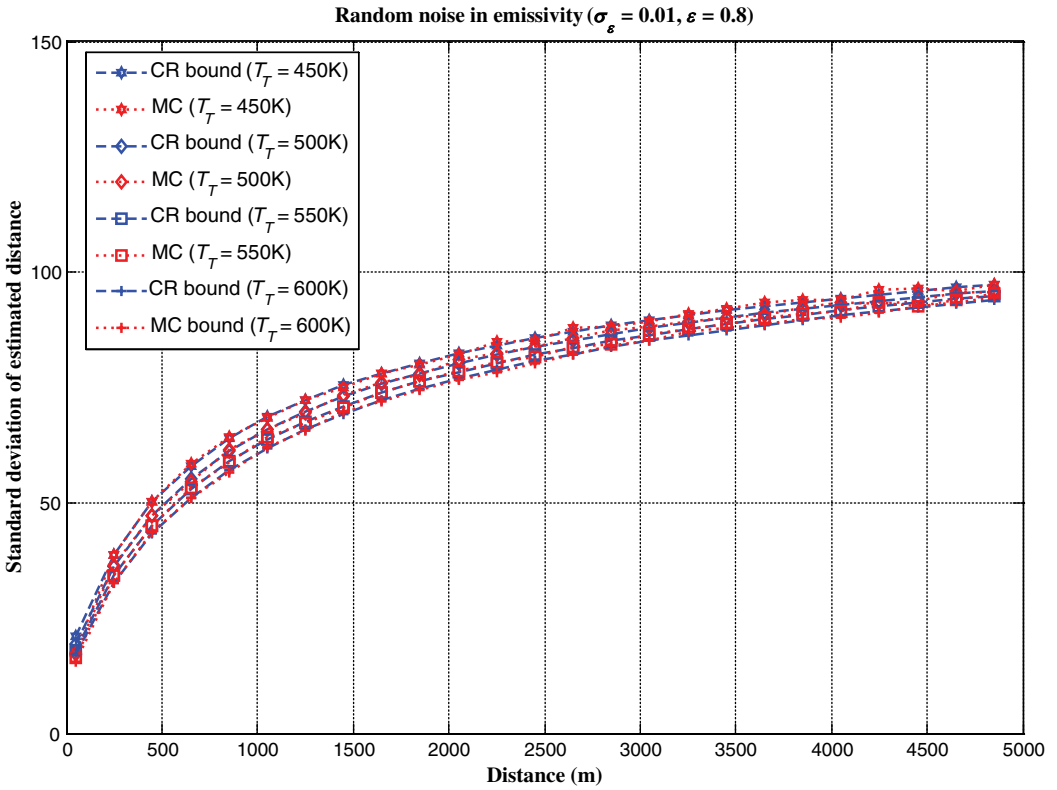


**Fig. 7** CRLB and standard deviation of ML estimated distance to distance curve in the emissivity uncertainty case, $T_T = 450$, 500, 550, and 600 K.

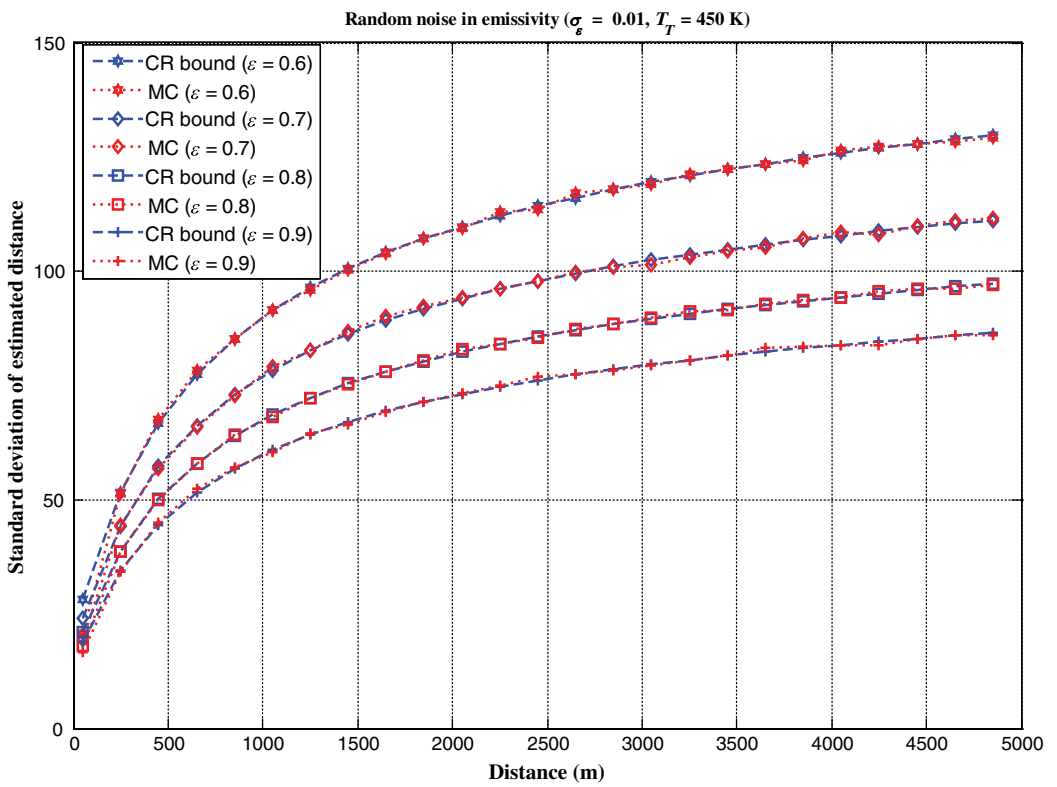


**Fig. 8** CRLB and standard deviation of ML estimated distance to distance curve in the emissivity uncertainty case, $e = 0.6$, 0.7, 0.8, and 0.9.

### 4.2 *Effect of Emissivity Uncertainty*

The average and variance of maximum likelihood estimator $d_{\mathrm{ML}}$ is also evaluated 20,000 times in Monte-Carlo simulation via various standard deviations in emissivity noise, target temperature, and emissivity. Although the mean and variance of the PDF is a nonlinear equation of the distance $d$ in Eq. (11), the results of Monte-Carlo simulation shown in Figs. 6–8 are converged to CRLB, and the maximum likelihood estimator of the distance is efficient. To evaluate the MLE solution $d_{\mathrm{ML}}$, we differentiate the log-likelihood function and set it equal to zero. Unlike the case of only thermal noise, it cannot be obtained from a simple linear equation and closed form. In Fig. 6, we see that the CRLB and the standard deviation of ML estimated distance to true distance curve for various emissivity noise standard deviations. As the standard deviation in emissivity noise $s_e$ increases, the standard deviation of estimated distance also increases, and the detection performance decreases. By comparing Figs. 4 and 5 with Figs. 7 and 8, we can see that target temperature and emissivity are insensitive to standard deviation of estimated distance in the case of emissivity noise. In short, as $s_e$ increases, the target temperature and emissivity decrease, and the standard deviation of estimated distance increases. Passive ranging gives reasonably accurate range estimation within a margin of error of 10% with a 95% confidence interval when the target temperature, range, standard deviation in emissivity noise, and emissivity are more than 500 K, 2000 m, 0.02, and 0.7, respectively.

## 5 Conclusion

In this paper, we propose the range estimation method using maximum likelihood estimation based on the atmospheric transmittance and atmosphere propagation-based radiance model. The fundamental limits of target range estimation are computed for various standard deviations in thermal and emissivity noise, target temperature, and emissivity. To analyze the performance of the proposed method, we evaluate the CRLB and Monte-Carlo simulation results. Because the solution of maximum likelihood estimation is an efficient estimator, the variance of the estimated target range is converged to the evaluated CRLB. In contrast with the case of thermal noise, the temperature and emissivity are insensitive parameters to the detection performance in the case of emissivity noise. Although there are many more uncertainties in the real environment, we find out the fundamental limits evaluated from CRLB are very dependent on thermal noise and emissivity uncertainty.

### *Acknowledgments*

This work was supported in part by the contracts ADD IIRC, 2011, and National Research Foundation of Korea (NRF) Grant funded by the Korean government (No. 2012M4A2026724).

### *References*

1. R. D. Hundson, *Infrared System Engineering*, pp. 62–91, John Wiley and Sons, New York (1969).
2. H. P. Wu and X. Yi, "Operating distance equation and its equivalent test for infrared search system with full orientation," *Int. J. Infrared Millim. Waves* **24**(12), 2059–2068 (2003).
3. L. Korba, S. Elgazzar, and T. Welch, "Active infrared sensors for mobile robots," *IEEE Trans. Instrument. Meas.* **43**(2), 283–287 (1994).
4. V. Colla and A. M. Sabatini, "A composite proximity sensor for target location and color estimation," in *Proc. IMEKO Sixth International Symposium on Measurement and Control in Robotics*, pp. 134–139, IMEKO, Brussels (1996).
5. A. M. Sabatini, V. Genovese, and E. Guglielmelli, "A low-cost, composite sensor array combining ultrasonic and infrared proximity sensors," in *Proc. IEEE/RSJ International Conference on Intelligent Robots and Systems (IROS)*, Vol. 3, pp. 120–126, IEEE, Pittsburgh, PA (1995).
6. A. Tofani, "Analysis of the infrared emission due to aerodynamic heating of missile domes," *Proc. SPIE* **1112**, 340–351 (1989).
7. A. Tofani, "Computer modeling of infrared head-on emission from missile noses," *Opt. Eng.* **29**(2), 87–96 (1990).
8. A. Berk et al., *MODTRAN4 Users Manual*, Air Force Geophysics Laboratory, Hanscom AFB, MA (2004).
9. P. T. Landsberg, "Bosons: black-body radiation," Chapter 13 in *Thermodynamics and Statistical Mechanics*, Courier Dover Publications, New York (1990).
10. D. A. Bell, *Noise and the Solid State*, Pentech, London (1985).
11. W. Bennett, *Electrical Noise*, McGraw-Hill, New York (1960).

Biographies and photographs of the authors are not available.